Pharmacokinetics of Topically Applied Pilocarpine in the Albino Rabbit Eye

MICHAEL C. MAKOID * and JOSEPH R. ROBINSON ˣ

Received February 23, 1978, from the *School of Pharmacy, University of Wisconsin, Madison, WI 53706.* Accepted for publication October 4, 1978. *Present address: College of Pharmacy, University of Nebraska Medical Center, Omaha, NB 68105.

Abstract □ The temporal and spatial pattern of [^{3}H]-pilocarpine nitrate distribution in the albino rabbit eye following topical administration was determined. A four-compartment caternary chain model describing this disposition corresponds to the precorneal area, the cornea, the aqueous humor, and the lens and vitreous. Simultaneous computer fitting of data from tissue corresponding to some compartments in the model supported the proposed model. Additional support was provided by the excellent correlation between predicted and observed values in multiple-dosing studies. Several important aspects of ocular drug disposition are evident from the model. The extensive parallel elimination at the absorption site gives rise to an apparent absorption rate constant that is one to two orders of magnitude larger than the true absorption rate constant. In addition, aqueous flow accounts for most of the drug removal. Thus, major effects on absorption and elimination, independent of the drug structure, suggest the possibility of similar pharmacokinetics for vastly different drugs.

Keyphrases □ Pilocarpine—distribution following topical administration, precorneal area, cornea, aqueous humor, lens, vitreous humor, rabbits, models □ Eye—pilocarpine distribution following topical administration, rabbits, models □ Models, pharmacokinetic—pilocarpine distribution following topical administration, eye

Until recently, the ocular disposition of topically applied pilocarpine was described with a one-compartment model. This model was satisfactory for short-term drug levels, but studies over longer times revealed significant deviation from the model (Fig. 1) (1–3).

Many ocular drugs of different physicochemical properties have strikingly similar pharmacokinetic profiles (4–8). The peak times and the absorption and elimination rate constants for these drugs are remarkably similar in view of the differences in drug properties and the complexity of the eye. Most drugs, when analyzed with a simple one-compartment model, appear to penetrate the cornea very rapidly. This rapid penetration from single doses differs from levels from multiple dosing of short duration and from sustained-release products. Maintenance of a high drug concentration in the lacrimal fluid for extended periods should significantly increase the amount of drug penetrating the eye if the penetration rate is rapid. This effect was found not to be the case (9).

The present study was designed to examine the disposition of topically administered pilocarpine in an attempt to clarify previous observations.

EXPERIMENTAL

Materials—Water was double distilled from alkaline permanganate solution in an all-glass apparatus.

Pilocarpine nitrate USP[1] was used without further purification. Tritiated pilocarpine nitrate[2], specific activity 4.1–6.95 Ci/mmole, was purified as previously described (10). Purity was established by paper chromatography and TLC. All other chemicals and reagents were either analytical or reagent grade and were used as received.

Male New Zealand albino rabbits[3], 1.8–2.4 kg, were used. Animals were individually housed in standard laboratory cages and were fed a regular diet with no restrictions on food or water.

Methods—*Solution Preparation*—Pilocarpine nitrate solutions, 5×10^{-4}–10^{-1} *M*, were prepared in 0.067 *M* Sorensen pH 6.24 phosphate buffer to which a small quantity of radioactive pilocarpine had been added. Solutions were made isoosmotic with tears by addition of sodium chloride, except in the 10^{-1} *M* case, which was already slightly hyperosmotic. In preparing the 5×10^{-4} *M* solutions, the amount of tritiated pilocarpine added was included when calculating the final solution molarity. For the remaining solutions, the small amount of tritiated pilocarpine did not influence the molarity of the final solution.

No attempt was made to induce or to maintain the sterility of the solutions, which were freshly prepared and discarded immediately after use. The final activity of the labeled tracer solutions varied depending on the duration of the experiment. The activity ranged from 0.025 mCi/ml (4×10^5 cpm/25 μl) in the short time periods to 1 mCi/ml (1.6×10^7 cpm/25 μl) in experiments lasting over 6 hr. Raw data in counts per minute were converted to micrograms of drug per milliliter of aqueous humor or per gram of tissue by use of an internal standard and standard radioisotope techniques.

Sampling Techniques—Pilocarpine solution, 25 μl, was instilled onto the animal cornea and collected in the cul-de-sac. For instillation, the lower lid was gently pulled away from the eye globe to form a pocket but was immediately returned to the normal position after drug instillation. In the multiple-dose study, this procedure was repeated at 30-min intervals for five doses. The animals were dosed upright in minimum restraining cages and were returned to their cages for the longer time periods.

At various postinstillation times, rabbits were sacrificed by rapid injection of an overdose of pentobarbital sodium into the marginal ear vein. A single puncture was then made, with a 27-gauge 1.25-cm needle, through the corneal-scleral junction into the anterior chamber. Aqueous humor, 100–200 μl, was aspirated from the anterior chamber and allowed to remain in the syringe until completion of the surgery, at which time

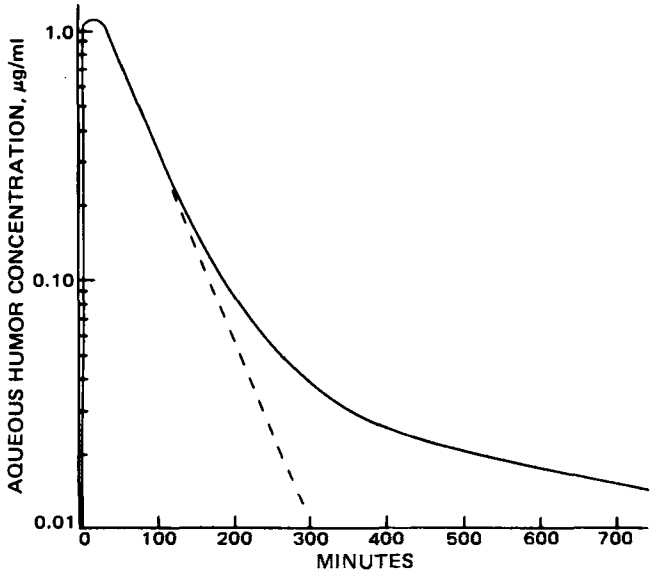

Figure 1—*Aqueous humor drug concentration* versus *time profile following topical administration of 25 μl of 10^{-2} M pilocarpine nitrate. The initial apparent one-compartment kinetics are shown as a dashed line, and deviations at longer time points are shown with a continuous line.*

[1] Merck & Co., Rahway, N.J.
[2] New England Nuclear, Boston, Mass.
[3] Klubertanz Rabbitry, Edgerton, Wis.

0022-3549/79/0400-0435$01.00/0

a 100-μl aliquot was transferred quantitatively by micropipet[4] from a planchet to a scintillation counting vial[5] containing 5 ml of scintillation fluid[6]. To minimize chemiluminescence, the liquid scintillation cocktail was refrigerated for at least 24 hr at 4° prior to transfer and counting. Solutions were read on a liquid scintillation counter[7].

After removal of aqueous humor, the eye was proptosed by inserting the handle of a scalpel behind the orb at the lateral (outer) canthus, and a straight Kelly clamp was placed under the orb at the medial (inner) canthus. A perilimbal incision was then made to a depth sufficient to sever the iris from the ciliary body. The cornea and iris were removed as a single unit, placed on a small filter paper, and gently blotted to remove excess fluid. The tissues were then separated and placed in preweighed combustion cones[8] for subsequent assay. The lens extruded during this procedure and was also placed in a preweighed combustion cone for analysis. The ciliary body was extracted from the sclera with vitreous humor attached.

By drawing the ciliary body between two sets of forceps, it was possible to remove the gel-like vitreous humor. Both tissues were then placed in preweighed combustion cones. All tissues were immediately weighed and allowed to air dry to facilitate oxidation. No significant difference could be detected between samples allowed to air dry prior to oxidation or oxidized wet. The tissue samples were introduced into a sample oxidizer[9] for analysis. Tritium was trapped as tritiated water in 10 ml of solvent[10]. These solutions were then equilibrated at 13° in the refrigerated scintillation counter for 6 hr prior to tritium assay.

The time between animal sacrifice and sampling should be minimal, especially at the earlier time points. Time for total surgery ranged from 1.5 to 2 min/eye.

At least eight determinations were made at each time point for each tissue. The various tissue–drug concentration *versus* time data fit a multicompartment model. After initial graphical estimates of the associated parameters, the profiles were subjected to computer analysis[11]. To determine the amount of pilocarpine in the various compartments, the data were converted to micrograms by multiplying the concentration in micrograms per milliliter by the estimated compartment size. The average cornea weighed 50 mg, the average iris and ciliary body weighed 20 mg each, the lens weighed 250 mg, the vitreous weighed 1 g, and the aqueous humor contained 250 μl. The absolute values of these compartments may vary by as much as 20%.

Stability Studies on Pilocarpine—*Chemical Analysis*—Intact pilocarpine was determined by the ferric hydroxamate method (11): 200 μl of 2.7 *N* NaOH, together with 200 μl of 2.5 *N* hydroxylamine hydrochloride, was spiked with 500 μl of the pilocarpine solution to be assayed. The solutions were allowed to react for 1 hr at room temperature or 4 min at 75°. Then 1.5 ml of 1.7 *M* ferric perchlorate in 0.8 *M* perchloric acid was added, and the resultant solution was allowed to react in the dark for 30 min. Finally, the solutions were brought to a volume of 7 ml with distilled water and read on a spectrophotometer[12] at 515 nm. The molar absorptivity of the solutions was 1.1×10^3 liters mole^{-1} cm^{-1}. This method produced a more stable color than previously reported, with an estimated fading rate of 15% in 24 hr.

Paper Chromatography—To determine the degradation and metabolic products of pilocarpine, various solutions and extracts were subjected to two-dimensional paper chromatography. The stationary phase was Whatman No. 4 paper; mobile phase one was *n*-butanol saturated with 0.1 *N* NH_4OH; mobile phase two was *n*-butanol saturated with 0.1 *N* HCl. The solvent front was allowed to proceed 10 cm in both directions, followed by drying of the paper and subsequent sectioning into 100 uniformly spaced squares. Each square was assayed for radioactivity, and the resulting R_f values were compared to known standards. Pilocarpic acid was prepared from intact pilocarpine by heating at 100° at pH 12 for 1 hr (12). In each case, only pilocarpine or pilocarpic acid could be shown to be present.

This procedure did not permit the detection of isopilocarpine, shown to be present by Sendelbeck *et al.* (13) using GLC. Tritiated pilocarpine was judged to contain 0.8% pilocarpic acid as a contaminant and to be stable with respect to lactone hydrolysis during the experiments. *In vitro* determinations of metabolites were carried out by incubating the iris and cornea in 1.0 ml of pilocarpine, 500 μg/ml, for various times and analyzing the solution for total pilocarpine by radioactive tracer analysis and for intact pilocarpine by spectral analysis.

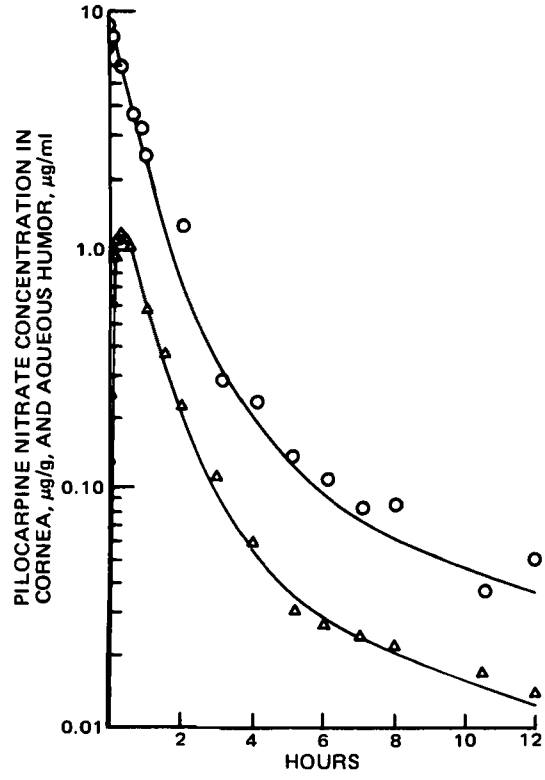

Figure 2—*Comparison of cornea* (○) *and aqueous humor* (△) *concentration data following instillation of 25 μl of* 10^{-2} M *pilocarpine nitrate with best-fit line generated by computer analysis.*

RESULTS

Degradation Studies—Intact pilocarpine was measured colorimetrically, and radioactive tracer analysis was used for total pilocarpine in determining the extent of pilocarpine degradation. Chromatography on *in vitro* incubates and *in vivo* ocular tissue homogenates identified degradation products. The metabolic rate was about 10^{-4} min^{-1}, in good agreement with the work of Sendelbeck *et al.* (13). The magnitude of this rate constant indicates significant differences between intact and total drug over time, *i.e.*, approximately 10–20% degradation over the 10–12 hr of the present study.

Drug Disposition Studies—*Tissue Drug Concentration* versus *Time Profiles from Single Dose*—Table I shows single-dose pilocarpine concentrations in various ocular tissues. The data for the 10^{-2} *M* pilocarpine were used for the primary analysis, with the results of other concentrations used as support. Cornea, C_c, and aqueous humor, C_{AH}, data from the 10^{-2} *M* dose were computer fitted to the four-compartment model equations (Fig. 2):

$$C_c = Ae^{-\alpha t} + Be^{-\beta t} + Ce^{-\Gamma t} + De^{-\Delta t} = \sum_{i=1}^{4} A_i e^{-\alpha_i t} \quad \text{(Eq. 1)}$$

$$C_{AH} = Ee^{-\alpha t} + Fe^{-\beta t} + Ge^{-\Gamma t} + He^{-\Delta t} = \sum_{i=1}^{4} A_i e^{-\alpha_i t} \quad \text{(Eq. 2)}$$

(Equation parameters are explained in the *Appendix*.)

Tissue Drug Concentrations versus *Time Profiles from Multiple Doses*—The multiple-dose tissue drug concentration *versus* time profiles are presented in Table II. The cornea and aqueous humor data were fitted to the four-compartment model multiple-dosing equations:

$$C_c = M\left[\sum_{i=1}^{4} \frac{A_i e^{-\alpha_i t}(1 - e^{-n\alpha_i \tau})}{(1 - e^{-\alpha_i \tau})}\right] \quad \text{(Eq. 3)}$$

$$C_{AH} = M\left[\sum_{i=1}^{4} \frac{A_i e^{-\alpha_i t}(1 - e^{-n\alpha_i \tau})}{(1 - e^{-\alpha_i \tau})}\right] \quad \text{(Eq. 4)}$$

where t equals the time since the last dose, τ is the time between doses, and M represents the lacrimal concentration buildup as explained pre-

[4] Biopette, Schwarz/Mann, Orangeburg, N.Y.
[5] Minivials, I.C.N., Irvine, Calif.
[6] Aquasol, New England Nuclear, Boston, Mass.
[7] Tri-Carb, Packard Instrument Co., Downers Grove, Ill.
[8] Combusto-Cones, Packard Instrument Co., Downers Grove, Ill.
[9] Packard model 306, Packard Instrument Co., Downers Grove, Ill.
[10] Monophase-40, Packard Instrument Co., Downers Grove, Ill.
[11] MACC subroutine NREG.
[12] Cary 16.

Table I—Tissue Drug Concentrations at Various Times following a Single Instillation of 25 μl of Pilocarpine Nitrate of Various Concentrations [a]

	Cornea				Aqueous Humor				Iris			
Minutes	10^{-1} M [b]	10^{-2} M	5×10^{-3} M	5×10^{-4} M	10^{-1} M [b]	10^{-2} M	5×10^{-3} M	5×10^{-4} M	10^{-1} M [b]	10^{-2} M	5×10^{-3} M	5×10^{-4} M
0.5		3.1 (11)				0.018 (16.7)						
2		7.0 (6)				0.017 (29)						
4		9.0 (5)				0.25 (8)				0.45 (12.4)		
6		8.8 (10)				0.6 (10)				0.67 (15)		
10		7.8 (16)				0.95 (4.7)				0.65 (20)		
20	21.2 (11)	6.0 (13)	2.2 (10)	0.29 (11)	5.7 (9.8)	1.2 (4.4)	0.71 (11)	0.076 (7.9)	4.8 (20)	1.1 (19)	0.54 (18)	0.129 (13)
30			0.87 (10)			1.1 (4.6)	0.46 (7.8)				0.16 (18)	
40		3.7 (13)										
50		3.2 (19)										
60	5.8 (8.2)	2.5 (9)	0.59 (11)	0.11 (12)	2.3 (8.8)	0.56 (7.7)	0.41 (6.6)	0.033 (12)	1.57 (6.4)	0.54 (20)	0.058 (9)	0.032 (16)
90						0.37 (8.6)						
120	3.8 (34)	1.2 (10)	0.25 (8)	0.025 (20)	1.3 (5.3)	0.22 (8.6)	0.13 (10)	0.0079 (8.9)	0.9 (30)	0.31 (9.7)	0.11 (11.5)	0.018 (22)
180		0.27 (10)				0.12 (11.3)				0.12 (11)		
240	0.5 (11)	0.22 (12)	0.15 (13)		1.6 (1.6)	0.059 (11.9)	0.022 (9.1)		0.32 (12.5)	0.073 (8.2)	0.029 (14)	
300		0.13 (9)				0.031 (22.8)				0.028 (14)		
360		0.10 (10)	0.098 (20)	0.0048 (17)	0.08 (6.3)	0.027 (7.9)	0.015 (13.3)	0.001 (10)	0.35 (22)	0.03 (33)	0.029 (21)	0.0015 (27)
420		0.075 (13)				0.024 (4.2)				0.026 (38)		
480	0.38 (20)	0.076 (12)		0.0038 (13)		0.022 (9.1)		0.00072 (10)	0.32 (29)	0.021 (19)		0.0007 (29)
600				0.0031 (16)				0.00065 (7.7)				0.0006 (21)
630		0.032 (3)				0.017 (5.9)						
720	0.27 (22)	0.043 (14)	0.029 (17)		0.09 (7.8)	0.014 (7.1)	0.008 (3.8)		0.22 (19)	0.016 (12.5)	0.022 (64)	

	Ciliary Body				Lens				Vitreous Humor			
Minutes	10^{-1} M [b]	10^{-2} M	5×10^{-3} M	5×10^{-4} M	10^{-1} M [b]	10^{-2} M	5×10^{-3} M	5×10^{-4} M	10^{-1} M [b]	10^{-2} M	5×10^{-3} M	5×10^{-4} M
0.5												
2						0.016 (25)				0.017 (23)		
4		0.3 (12)				0.017 (12)				0.024 (17)		
6		0.56 (21)				0.024 (8)				0.018 (28)		
10		0.50 (22)				0.017 (24)				0.029 (14)		
20	3.7 (13.5)	1.2 (19)	0.37 (12)	0.031 (16)	0.32 (15)	0.04 (12)	0.025 (8)	0.005 (16)	0.38 (29)	0.040 (18)	0.044 (27)	0.003 (37)
30							0.022 (14)				0.12 (17)	
40												
50												
60	1.1 (12)	0.38 (13)	0.11 (14)	0.036 (42)	0.22 (10)	0.058 (14)	0.012 (8.3)	0.005 (10)	0.26 (18)	0.028 (14)	0.004 (25)	0.0027 (37)
90												
120	0.64 (28)	0.19 (27)	0.071 (14)	0.01 (15)	0.19 (31)	0.047 (11)	0.024 (17)	0.003 (16)	0.078 (22)	0.032 (28)	0.0077 (39)	0.0005 (40)
180		0.09 (11.1)				0.039 (13)				0.021 (24)		
240	0.39 (21)	0.11 (18)	0.049 (63)		0.2 (9)	0.051 (16)	0.014 (11)		0.047 (30)	0.010 (20)	0.0067 (49)	
300		0.033 (30)				0.016 (6)				0.005 (20)		
360	0.24 (11)	0.033 (24)	0.043 (81)	0.0008 (36)	0.072 (20)	0.033 (9)	0.011 (9)	0.0011 (9)	0.035 (17)	0.015 (40)	0.006 (25)	0.00033 (21)
420		0.016 (13)				0.02 (20)				0.006 (33)		
480	0.19 (21)	0.029 (28)			0.14 (14)	0.021 (9)		0.00015 (7)	0.032 (9)	0.016 (31)		0.0005 (41)
600				0.0004 (29)				0.00010 (9)				0.00048 (8)
630		0.013 (62)				0.01 (10)				0.01 (20)		
720	0.091 (37)	0.014 (29)	0.014 (64)		0.061 (23)	0.01 (10)	0.0077 (14)		0.030 (23)	0.005 (20)	0.0027 (22)	

[a] Calculations are based on pilocarpine nitrate, although it is probable that pilocarpine is being measured. Concentrations are defined as micrograms of pilocarpine nitrate per gram of wet tissue or per milliliter of aqueous humor. Standard error of the mean is expressed as a percent of the value determined and is shown in parentheses. The number of eyes ranged between eight and 37 per time point. [b] Toxic manifestations, *e.g.*, copious lacrimation, occurred at this level. Accuracy of the numbers is, therefore, questionable.

Table II—Drug Concentration during Multiple Dosing of 25 μl of 10^{-2} *M* Pilocarpine Nitrate Every 0.5 hr for a Total of Five Doses [a]

Minutes	Cornea	Aqueous Humor	Ciliary Body	Iris	Lens	Vitreous Humor
45	8.4 (5.1)	2.4 (7.4)	0.91 (9.1)	1.4 (2.2)	0.13 (2.2)	0.033 (12)
60	3.8 (6.3)	2.0 (14.7)	0.74 (21)	1.0 (17)	0.10 (15)	0.039 (24)
75	19.0 (1.1)	1.9 (4.6)	2.4 (12)	2.9 (7.8)	0.18 (9)	0.12 (23)
90	5.9 (6.3)	3.3 (21)	1.9 (22)	2.9 (7.2)	0.16 (16)	0.13 (21)
105	15.0 (11)	5.8 (12)	2.7 (25)	3.0 (13)	0.27 (42)	0.10 (81)
120	15.0 (6.1)	5.1 (12)	2.2 (15)	3.6 (8.1)	0.27 (6)	0.11 (20)
135	14.0 (10)	3.4 (23)	2.9 (13)	5.2 (8.9)	0.26 (15)	0.26 (20)
150	14.0 (10)	2.5 (24)	2.2 (14)	2.6 (20)	0.19 (14)	0.090 (18)
165	7.0 (10)	3.0 (6.6)	1.7 (14)	1.9 (6.8)	0.18 (12)	0.051 (12)
180	4.4 (16)	1.9 (16)	1.1 (28)	1.4 (15)	0.22 (19)	—
240	2.1 (32)	0.64 (16)	0.4 (39)	0.73 (15)	0.13 (16)	0.051 (34)
300	2.1 (24)	0.38 (9.3)	0.45 (25)	0.68 (12)	0.16 (17)	0.070 (26)
360	0.82 (29)	0.23 (10)	0.13 (11)	0.15 (22)	0.12 (22)	0.030 (13)
480	0.52 (28)	0.14 (412)	0.10 (23)	0.11 (26)	0.08 (25)	0.033 (24)

[a] Concentrations are micrograms of drug per gram of wet tissue. Standard error of the mean is expressed as a percent of the value determined and is shown in parentheses; $n \geq 8$.

viously (14, 15). A more complete program is currently under investigation. The results of the equation fitting are shown in Figs. 3 and 4.

DISCUSSION

Drug Disposition Studies—Only the model shown in Scheme I gave simultaneous fit to both cornea and aqueous data ($r > 0.99$). The pharmacokinetic parameters generated by computer fitting are shown in Table III.

Two- or three-compartment caternary models gave reasonable correlation coefficients ($r \approx 0.9$), but major portions of the data had to be ignored in the fitting process. More complex models also gave good fit to the data, but there was no compelling reason to adopt them. The four-compartment model was selected partly because anatomical significance could be attributed to the various compartments.

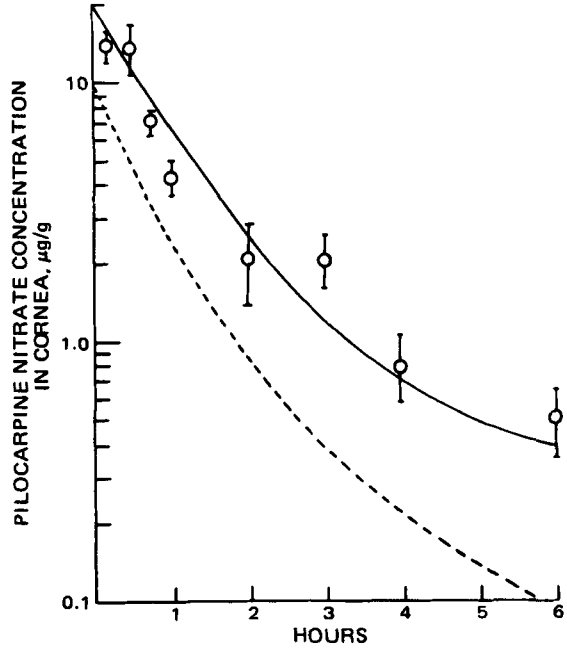

Figure 3—*Concentration of pilocarpine nitrate in the cornea (O) as a function of time after the last dose as compared with the calculated (—) multiple-dose line using Eq. 3. The single-dose line (– –) generated by the four-compartment model is drawn in for comparison.*

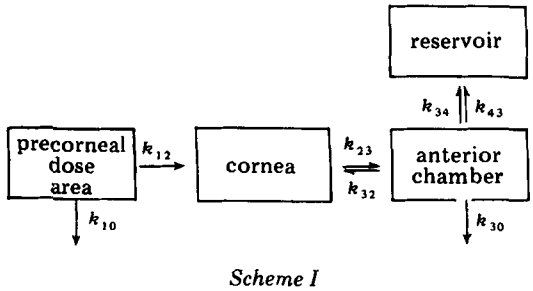

Scheme I

These data and the proposed model explain some previously anomalous findings. The observations that many drugs are rapidly absorbed across the cornea and that drugs with dissimilar physical-chemical properties show similar corneal absorption profiles (4–8) can be explained by recognizing the importance of the precorneal elimination pathway, k_{10}, on corneal absorption. Several investigators (1–3) commented recently that the cornea is not a simple semipermeable membrane. Aqueous humor drug studies of short duration frequently produced a biphasic curve of drug level *versus* time, which led to a simplistic view of the cornea. The idea that drugs diffused from lacrimal fluid through the "membrane" of the cornea into the aqueous humor led to the erroneous conclusion that the absorption rate constant obtained from such studies represented drug transfer from the tears to the aqueous humor. Studies of longer duration showed the disposition pattern of drug in both the cornea and aqueous humor to be more complex.

Drug contact time from 0 to 5 min postinstillation has been shown to be critical for drug absorption into the cornea and aqueous humor (16). The early peak time in the cornea led to the assumption of an erroneously large absorption rate constant of 0.5–0.7 min^{-1}. The early peak times in the cornea and aqueous humor are due to rapid elimination from the precorneal area and a rapid decrease in the concentration gradient between the tears and the cornea surface.

The influence of parallel elimination from an absorption site on the pharmacokinetic parameters obtained has been described (17–20). The simplest pharmacokinetic model for the eye is the single-compartment model (Scheme II). A more appropriate model, incorporating the parallel elimination step from the precorneal area, is shown in Scheme III.

Table III—Pharmacokinetic Parameters [a] Obtained by Fitting Data Generated from a Single 25-μl Dose of 10^{-2} *M* Pilocarpine Nitrate to Four-Compartment Model Equations [b] for Cornea and Aqueous Humor

Parameter	Cornea		Aqueous Humor	
	Concentration	Amount	Concentration	Amount
A_1[c]	−12	−0.61	0.41	0.10
A_2[c]	+0.20	+0.01	0.077	0.019
A_3[c]	4.3	0.22	−2.4	0.6
A_4[c]	7.7	0.39	1.9	0.47
α_1, min^{-1}	0.58	0.58	0.58	0.58
α_2, min^{-1}	0.0026	0.0026	0.0026	0.0026
α_3, min^{-1}	0.11	0.11	0.11	0.11
α_4, min^{-1}	0.019	0.019	0.019	0.019
AUC[d]	510	25.9	210	27
Peak time, min	4	4	20	20
r^2	0.99+	0.99+	0.99+	0.99+
r	0.99+	0.99+	0.99+	0.99+

[a] All parameters were allowed to float free to obtain best fit by nonlinear regression analysis of simultaneous aqueous humor and corneal data. [b] $C_C = Ae^{-\alpha t} + Be^{-\beta t} + Ce^{-\Gamma t} + De^{-\Delta t}$, and $C_{AH} \approx Ee^{-\alpha t} + Fe^{-\beta t} + Ge^{-\Gamma t} + He^{-\Delta t}$. Derivation of these equations are shown in the *Appendix*. [c] Corneal concentration equals micrograms per gram, aqueous humor concentration equals micrograms per milliliter, and amount equals micrograms. [d] Area under the curve in concentration (or amount units) × minutes.

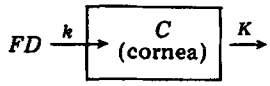

Scheme II

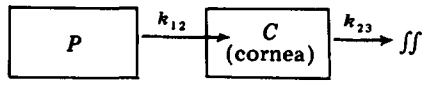

Scheme III

The equations describing these processes in terms of drug amounts are:

$$C = (FD)\left(\frac{k}{k-K}\right)(e^{-Kt} - e^{-kt}) \qquad \text{(Eq. 5)}$$

for Scheme II, where F is the fraction of the dose absorbed and D is the dose, and:

$$C = \left(\frac{Dk_{12}}{k_{12}+k_{10}-k_{23}}\right)[e^{-k_{23}t} - e^{-(k_{12}+k_{10})t}] \qquad \text{(Eq. 6)}$$

for Scheme III.

Since $F = k_{12}/(k_{12}+k_{10})$, it is obvious that $K = k_{23}$ and $k = k_{12}+k_{10}$; or, in other words, the absorption rate constant into the compartment monitored (Scheme II) is the summation of the elimination rate constants from the previous compartments. The first implication of this analysis is that the fraction of drug absorbed bears directly on the apparent absorption rate constant. Since the apparent rate constant is proportional to $1/F$, multiplication of the apparent rate constant by F should result in an approximation of the true rate constant; *i.e.*, $F \times k_{apparent} = k_{true}$. This is borne out by analysis of the initial corneal data, *i.e.*, less than 2 hr. The apparent absorption rate constant in this case is 0.62 min^{-1}, which, when multiplied by $F \approx 1$–2%, yields 6–12 $\times 10^{-3}$ min^{-1}. Computer estimate of k_{12} is 6.2 $\times 10^{-3}$ min^{-1}, in excellent agreement with the proposed model.

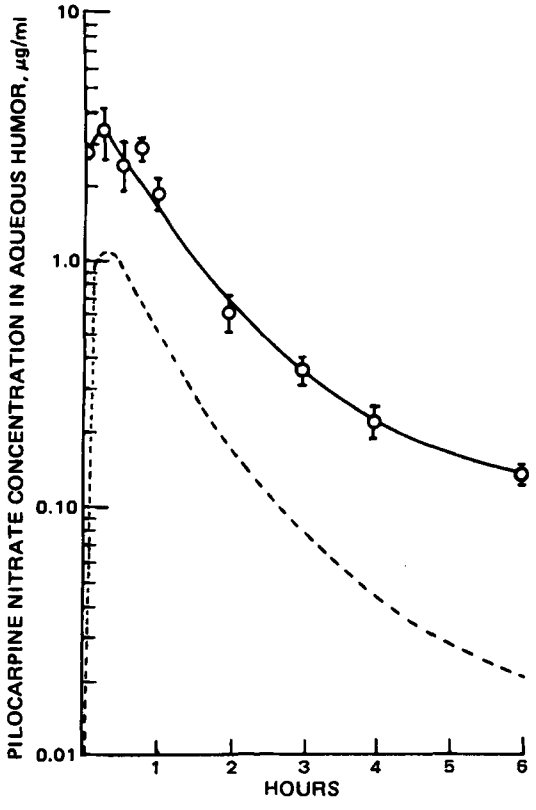

Figure 4—*Concentration of pilocarpine nitrate in the aqueous humor (○) as a function of time after the last dose as compared with the calculated (—) multiple-dose line using Eq. 4. The single-dose line (– –) generated by the four-compartment model is drawn in for comparison.*

Table IV—Bioavailabilities of Drug in the Aqueous Humor and Cornea after Rinsing at Various Times

Rinse Time Postinstillation, min	Percent Bioavailable[a]	Aqueous[b] Humor	Cornea[c]
0.5	33	33	34
1	—	55	—
2	75	80	78
3	—	91	—
4	—	100	100
5	100	100	100
No rinse	100	100	100

[a] Percent maximum miosis peak height (14). [b] Percent maximum area under the curve (16). [c] Percent maximum concentration.

The second implication is that peak time is:

$$T_p = \frac{\ln\left(\frac{k_{12}+k_{10}}{k_{23}}\right)}{k_{12}+k_{10}-k_{23}} \qquad \text{(Eq. 7)}$$

If $k_{10} \gg k_{12}$, then:

$$T_p = \frac{\ln\left(\frac{k_{10}}{k_{23}}\right)}{k_{10}-k_{23}} \qquad \text{(Eq. 8)}$$

This means that F approaches zero, k_{10} approaches infinity, and T_p approaches zero. The T_p value is relatively insensitive to k_{23} and k_{12}; *e.g.*, at small F, a 100-fold change in k_{23} results in a threefold change in T_p, and k_{12} must approach k_{10} to have a significant effect on T_p. Consequently, T_p would be similar even for dissimilar drugs because of the overshadowing of k_{12} and k_{23} by k_{10}.

This analysis also explains aqueous humor drug concentrations observed by Patton (9), who blocked the drainage ducts of rabbits, thus effectively reducing k_{10}. He observed a modest shift in peak time and a two- to threefold increase in the area under the curve (*AUC*), both of which are consistent with this model.

Corneal drug absorption ceases at 4–5 min postinstillation due to a very

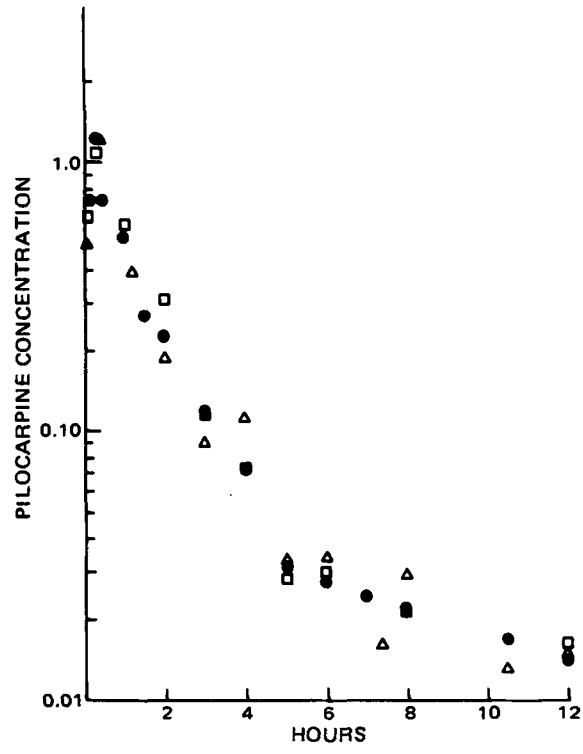

Figure 5—*Comparison of iris (□) and ciliary body (△) concentrations following a single dose of 25 μl of 10^{-2} M pilocarpine nitrate with aqueous humor data (●). Aqueous humor drug concentrations are in micrograms per milliliter; for the other tissues, drug concentration is in micrograms per gram wet weight tissue. Error bars are omitted for clarity.*

Table V—Pilocarpine in All Tissues Based on Area under the Curve Calculations and Estimated Tissue Size

Observed Parameter	Cornea	Aqueous Humor	Ciliary Body	Iris	Lens	Vitreous
Model size, mg	50	250	20	20	250	1000
Observed size, mg ($\bar{x} \pm SEM$, $n = 100$)	53.1 ± 0.8	300	20.7 ± 6.2	19.7 ± 7.3	257 ± 48	1077 ± 9.3
AUC, μg-min	25.4	27.2	2.17	2.17	6.4	11.82
Amount, μg	0.75	0.8	0.064	0.064	0.19	0.35
Instilled dose, %	1.1	1.2	0.1	0.1	0.28	0.52
Relative absorbed dose, %	100	110	8.8	8.8	26	48

large precorneal elimination rate constant and substantial drug accumulation at the corneal surface, as shown by the drug levels in the tears and the cornea at 4–5 min.

The cornea consists of two main tissue types, the lipophilic epithelium and the hydrophilic stroma, which have considerably different drug absorption and transport characteristics (16). The principal barrier and depot for pilocarpine, and presumably many ocular drugs, is in the epithelium. Movement of water-soluble drug through the stroma is usually rapid, with diffusion coefficients similar to those in water. Consequently, the cornea can be treated as two subcompartments, the epithelium and the stroma, assuming that the endothelium, a single layer of cells intermediate in properties between the lipophilic epithelium and hydrophilic stroma, is not rate limiting. Because of the facility of pilocarpine movement through the stroma, it can be combined with the aqueous humor, effectively reducing the cornea to a single compartment, the epithelium.

Since most of the drug present in the cornea is in the epithelial layer, the drug concentration at the cornea–tear interface is considerably higher than the average drug level in the cornea would indicate (16). At 5–6 hr postinstillation, the drug concentration in the cornea is three times that in the aqueous humor (stroma) (Fig. 2). Stated differently, the lipophilic epithelium contains 75% of the drug in approximately 10% of the corneal volume whereas the hydrophilic stroma contains 25% of the drug in 90% of the corneal volume. Use of this ratio to examine the 9-μg/g peak corneal drug concentration from a 10^{-2} *M* pilocarpine nitrate solution gives the ratio of drug between the epithelium and stroma:

$$\frac{\text{epithelium}}{\text{stroma}} = \left(\frac{75\% \times 9\ \mu g/g}{10\%}\right) \Big/ \left(\frac{25\% \times 9\ \mu g/g}{90\%}\right) = \frac{67.5\ \mu g/g}{2.5\ \mu g/g} \quad \text{(Eq. 9)}$$

Since the 3:1 ratio was obtained at 5–6 hr postinstillation while the corresponding ratio was much higher (~30–50:1) at times before the peak corneal drug level, these figures must be multiplied by 10–15 to give an average drug concentration in the epithelium of between 675 and 1000 μg/g. To average between 675 and 1000 μg/g in the epithelium during the first few minutes postinstillation, the drug concentration at the epithelial–tear surface would have to be twice that at the epithelial–stroma surface or between 1300 and 2000 μg/g.

Similarly, one can calculate the tear drug concentration. The following equation was modified from earlier work (14, 15):

$$C_L = \left(\frac{A_0}{V_0 + V_A}\right) \exp\left[-\left(\frac{0.66}{V_L + V_0 e^{-kt}} + k_n\right)t\right] \quad \text{(Eq. 10)}$$

where:

C_L = lacrimal concentration
A_0 = amount instilled
V_0 = volume instilled
V_L = resident lacrimal volume
V_A = apparent lacrimal volume due to volume of drop drained out undiluted
k_d = volume-dependent drainage rate constant
k_n = rate constant for nonproductive absorption

Solving Eq. 10 for a 25-μl drop gives a lacrimal drug concentration at 4 min of 1400 μg/ml, *i.e.*, approximately equal to that at the epithelial–tear interface at the same time (1300–2000 μg/ml). This explains the apparently large k_{10}, when no other process in the eye is of the magnitude necessary to shut down around 4 min. This apparent discrepancy is because flux is concentration dependent whereas present models are built on amount relationships.

On the basis of this analysis, flux should stop at about 4 min postinstillation and actually reverse at later times. Since this reverse flux is dependent not only on a small concentration difference but also on a very small first-order rate constant, the actual transfer rate out of the cornea should be very small. In fact, studies designed to show lacrimal drug concentration after dosing and subsequent flushing with saline failed to show detectable amounts of drug coming out of the cornea. Although the transfer between the precorneal fluid and the cornea is depicted as irreversible, it is probably reversible but not enough to interfere with the accuracy of the model.

The rapid decline in the lacrimal fluid–corneal surface concentration gradient results in apparent nonsink kinetics onto or into the cornea, as was demonstrated by initial corneal uptake studies (16). These studies, which determine relative pilocarpine bioavailability, correspond nicely with data from miosis studies (14) and with corneal absorption (Table IV). Thus, inclusion of the cornea as a component in the scheme of drug movement from the precorneal fluid into the anterior chamber explains the large apparent k_a and accounts for drug absorption into the aqueous humor even after the drug has been removed from the precorneal area. The corneal epithelium acts as a depot for drugs because it has significant volume and is not a simple semipermeable membrane.

Once the drug penetrates the cornea and enters the aqueous humor, it distributes throughout the eye. The anterior chamber is in intimate contact with the cornea, iris, ciliary body, lens, and vitreous. Rapid drug distribution to these areas is apparent from the iris and ciliary body data. Because of the lack of barrier epithelium and the open meshwork of connective tissue making up the iris and ciliary body, the drug concentration in these tissues mirrors that in the aqueous humor (Fig. 5). For pilocarpine disposition in albino rabbits, where pigment binding is absent, the anterior chamber compartment consists of the aqueous humor, iris, and ciliary body. Further work using pigmented strains will determine whether the iris and ciliary body drug disposition profiles also follow aqueous humor levels. Pigmentation is expected to significantly affect the amount of drug present in the iris (21).

The data show ~75% of the absorbed drug passing into the lens and vitreous reservoirs, as predicted by the model (Table V). The lens and vitreous data are fitted to a biexponential curve for preliminary treatment (Table VI). These preliminary data show that a portion of the drug becomes associated with the lens. The concentration gradient of drug within the lens has yet to be determined. Initial studies indicated that a substantial concentration gradient exists between the interior and exterior portions of the lens. Since the drug first penetrates the anterior chamber, the ventral surface of the lens should have a high drug concentration unless there is facile transport of drug around the lens. Thus, a critical examination of drug disposition in the lens needs to be conducted.

Transport into the vitreous humor also should be considered. The discrete anatomical tissue, the fibrils, comprising approximately 2% of the vitreous humor, should not hinder diffusion of relatively small molecules through the fluid space. Thus, microviscosity, rather than macroviscosity, should determine the diffusion rate. If this were the case, diffusion throughout the vitreous would be relatively rapid and the concentration gradient within the vitreous would be relatively shallow. Moreover, the peak time of drug in the vitreous would correspond closely to the aqueous humor peak time, which appears to be the case (Tables III and VI).

Table VI—Pharmacokinetic Parameters [a] Obtained by Fitting Lens and Vitreous Data to the Single-Compartment Model Equation, $Y = Ae^{-\alpha t} - Be^{\beta t}$, following a Single Instillation of 25 μl of 10^{-2} *M* Pilocarpine Nitrate

Parameter	Lens		Vitreous
	Concentration	Amount	Concentration [b]
A [c]	0.075	0.019	0.036
B [b]	0.071	0.018	0.037
α, min^{-1}	0.0027	0.0027	0.003
β, min^{-1}	0.037	0.037	0.21
AUC [d]	25	6.4	12
Peak time, min	76 min	76 min	21
r^2	0.96+	0.96+	0.97+
r	0.98+	0.98+	0.93+

[a] All parameters were allowed to float free to obtain best fit by nonlinear regression analysis. [b] The equation for the amount data is numerically identical because vitreous is 1 g; however, the units differ. [c] Lens and vitreous concentration equal micrograms per gram, and amount equals micrograms. [d] Area under the curve units: area concentration (or amount units) × minutes.

Table VII—Pharmacokinetic Parameters of Biphasic Decline of Aqueous Humor and Corneal Concentration Data Fit to the Equation $C = Ae^{-\alpha t} + Be^{-\beta t}$ following Instillation of 25 μl of Various Concentrations of Pilocarpine Nitrate

Parameter	Cornea				Aqueous Humor			
	10^{-1} M	10^{-2} M	5×10^{-3} M	5×10^{-4} M	10^{-1} M	10^{-2} M	5×10^{-3} M	5×10^{-4} M
Best Fit: All Parameters Allowed to Float Free								
A, μg/g	39.0	9.3	4.5	0.48	8.0	1.7	0.86	0.12
B, μg/g	1.1	0.48	0.070	0.0070	0.087	0.053	0.0083	0.0013
α, min^{-1}	0.034	0.24	0.016	0.026	0.02	0.019	0.016	0.023
β, min^{-1}	0.0030	0.0040	0.0060	0.0010	—	0.0039	—	0.0045
$A + B$, μg/g	40	9.8	4.6	0.49	8.1	1.8	0.87	0.12
AUC, μg/g min	1500	500	290	25	—	120	—	6.3
r^2	0.98+	0.99+	0.99+	0.99+	0.99+	0.99+	0.98+	0.99+
r	0.99+	0.99+	0.99+	0.99+	0.99+	0.99+	0.98+	0.99+
Constrained Fit: α and β Fixed to 10^{-2} M Exponents								
A, μg/g	28	9.3	4.6	0.43	7.6	1.7	0.92	0.1
B, μg/g	1.1	0.48	0.26	0.016	0.17	0.053	0.28	0.012
α, min^{-1}	0.024	0.024	0.024	0.024	0.019	0.019	0.019	0.019
β, min^{-1}	0.0040	0.0040	0.0040	0.0040	0.0039	0.0039	0.0039	0.0039
$A + B$, μg/g	29	9.8	4.8	0.45	7.7	1.8	0.95	0.1
AUC, μg/g min	3000	500	250	25	496	122	64.0	6.0
r^2	0.97+	0.99+	0.88+	0.99+	0.99+	0.99+	0.98+	0.99+
r	0.99−	0.99+	0.91+	0.99+	0.99+	0.99+	0.98+	0.99+

Most drug removal from the internal eye is *via* bulk flow of aqueous humor, although systemic loss *via* the vascular bed also occurs. Metabolism of the drug by ocular enzymes will be considered more fully in a subsequent publication.

This picture of drug removal is consistent with previous observations that the elimination rate for pilocarpine is significantly smaller than the aqueous flow rate (3), suggesting that:

1. Permeation from the cornea to the aqueous is slow so that the cornea becomes a depot for the drug, or
2. Iris tissue and its pigments bind the drug, forming a deep depot, or
3. Receptor dissociation occurs at a slow rate.

The fact that the data from albino rabbits without pigmented irides showed similar kinetics to the data from pigmented irides (3) indicates that tissue pigments may not be the dominant cause of deviation from simple one-compartment kinetics. The amounts of drug in the iris are not sufficient to maintain aqueous humor levels for an extended time. The cornea may modify pilocarpine penetration (22). Lazare and Horlington (1) showed an elimination phase in tissue samples that does not fit a simple biexponential equation, but they rejected the cornea as a drug reservoir. The deviation from simple kinetics may be due to distributive aspects, as in the present findings.

Both the corneal reservoir and drug equilibration from the vitreous humor are viable explanations of the pharmacokinetics, and both approaches are mathematically necessary to reproduce the curves simultaneously generated by the cornea and aqueous humor data. The "absorption and elimination rate constants" previously generated from the simple one-compartment model were only part of the story. They are a compilation of the various ongoing processes in the whole system (see *Appendix*), dominated by an apparent parallel elimination in the precorneal area and a distribution in the aqueous humor, with neither process especially dependent on the drug structure.

Testing the Model—*Concentration Dependence*—Consistency of the concentration-independent model would be evident if various concentrations of a drug generated a family of curves with similar slopes. The peak concentrations, AUC, and the intercept of the concentration axis in a semilogarithmic plot should be proportional to concentrations. Since the data collection for the absorption phase was complete only for the 10^{-2} M study, only the elimination phase was compared in all studies, using the 10^{-2} M study as the reference.

The results of these calculations (Tables VII and VIII) bear out the hypothesis ($r > 0.98$). The 10^{-1} M solution caused excessive lacrimation and a larger k_{10}, which was reflected in the decrease in drug uptake. This result is consistent with previous findings that aqueous humor drug concentrations over a large instilled fluid concentration range produce a linear relationship over several orders of magnitude (10).

Multiple-Dose Studies—Multiple-dosing studies were conducted at 0.5-hr dosing intervals to ensure integrity of the label and to get a sufficient amount in the reservoirs to show significant differences.

The model predicts a certain amount of drug buildup in ocular tissues due to deposition and equilibration of the drug in the aqueous humor with these tissues. There is excellent correlation between prediction and observation (Figs. 3 and 4) for both the cornea and aqueous humor. What the model does not predict, however, is the buildup of the precorneal concentration due to the previous dose. When the concentration in the precorneal area drops to that of the corneal epithelium, flux into the cornea ceases, even though there is still a significant amount of drug in the cul-de-sac. Upon addition of a second dose within a short period, dilution with tears does not have as much effect on incoming drug due to the presence of drug remaining from the previous dose. This buildup has been incorporated into the mathematics for multiple dosing of short τ.

The stepwise buildup of drug in all tissues is clear from Table II. The peak drug level shifted to longer times, which is normal in dosing intervals

Table VIII—Pharmacokinetic Parameters of Monophasic Decline of Lens and Vitreous Concentration Data Fit to the Equation $C = Ae^{-\alpha t}$ following Instillation of 25 μl of Various Concentrations of Pilocarpine Nitrate

Parameter	Lens				Vitreous Humor			
	10^{-1} M	10^{-2} M	5×10^{-3} M	5×10^{-4} M	10^{-1} M	10^{-2} M	5×10^{-3} M	5×10^{-4} M
Best Fit: All Parameters Allowed to Float Free								
A, μg/g	0.17	0.073	0.020	0.005	0.14	0.036	0.0099	0.0039
α, min^{-1}	0.0016	0.0027	0.0011	0.0033	0.0013	0.0031	0.0019	0.013
AUC, μg/g min	110	27	17	1.6	110	12	5.2	0.30
r^2	0.88	0.98	0.79	0.96	0.47	0.93	0.45	0.91
r	0.94	0.99	0.89	0.98	0.64	0.98	0.53	0.94
Constrained Fit: α Fixed to 10^{-2} M Exponent								
A, μg/g	0.21	0.073	0.032	0.0046	0.19	0.036	0.012	0.0025
α, min^{-1}	0.0027	0.0027	0.0027	0.0027	0.0031	0.0031	0.0031	0.0031
AUC, μg/g min	79	27	12	1.8	60	12	4.0	8.0
r^2	0.78	0.98	0.50	0.95	0.44	0.93	0.48	0.84
r	0.92	0.99	0.78	0.97	0.63	0.98	0.56	0.85

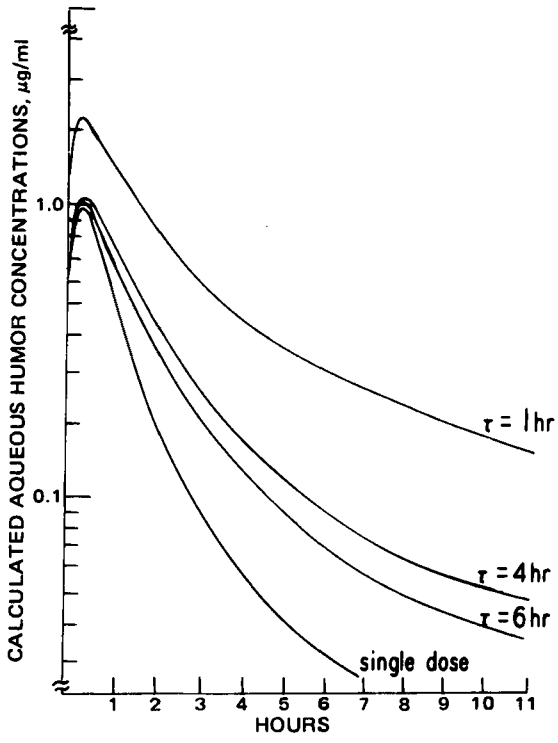

Figure 6—*Calculated aqueous humor levels* (n = ∞) *based on different dosing intervals* (τ).

of a short duration. Continuation of the dosage regimen would eventually cause a plateauing effect at a higher level than the original. Once drug in the reservoirs became significant, the overall shape of the curve changed (Fig. 6).

After a sufficient number of doses, the term $1 - e^{-n\alpha_i\tau}$ in Eqs. 3 and 4 goes to one. Consequently, at long-term maintenance:

$$C = M\left[\sum_{i=1}^{4}\frac{A_i e^{-\alpha_i\tau}}{(1-e^{-\alpha_i\tau})}\right] \qquad \text{(Eq. 11)}$$

With this equation, it is possible to generate the family of curves for varying dosing intervals (Fig. 6).

The model predicts a negligible increase in peak height at $n \to \infty$ for large τ (dosing intervals of 4–6 hr are normal) but significant increases in the amount remaining at the end of the dosing interval, showing an apparent reduction in the elimination rate constant. The increase in drug concentration is two to three times higher than the single-dose information in a properly designed experimental model (quadexponential) and several orders of magnitude higher in the biexponential model, which is currently being used in ocular pharmacokinetics.

APPENDIX

The mathematical derivation of the pharmacokinetic model for pilocarpine in the rabbit eye is as follows. Drug distribution in the eye can be compartmentalized as shown in Scheme IV:

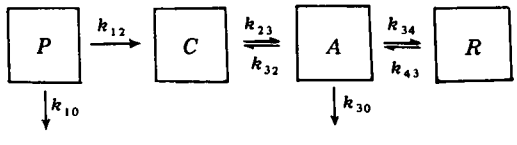

Scheme IV

where P is the precorneal area, C is the cornea, A is the anterior segment (excluding lens and cornea), R is the reservoir consisting of the lens and vitreous, and k_{ij} is the rate constant for drug transport into and out of the various areas.

By using standard matrix theory, it can be shown that the equations for concentrations in cornea, aqueous, and reservoirs are:

$$\text{cornea} = C_c = Ae^{-\alpha t} + Be^{-\beta t} + Ce^{-\Gamma t} + De^{-\Delta t} \qquad \text{(Eq. A1)}$$

$$\text{aqueous} = C_a = Ee^{-\alpha t} + Fe^{-\beta t} + Ge^{-\Gamma t} + He^{-\Delta t} \qquad \text{(Eq. A2)}$$

$$\text{reservoir} = C_R = Ie^{-\alpha t} + Je^{-\beta t} + Ke^{-\Gamma t} + Le^{-\Delta t} \qquad \text{(Eq. A3)}$$

where:

$$A = [(\text{dose/volume})k_{12}(XA-\alpha)(XB-\alpha)]\div[(\Gamma-\alpha)(\Delta-\alpha)(\beta-\alpha)]$$
$$B = [(\text{dose/volume})k_{12}(XA-\beta)(XB-\beta)]\div[(\Gamma-\beta)(\Delta-\beta)(\alpha-\beta)]$$
$$C = [(\text{dose/volume})k_{12}(XA-\Gamma)(XB-\Gamma)]\div[(\beta-\Gamma)(\Delta-\Gamma)(\alpha-\Gamma)]$$
$$D = [(\text{dose/volume})k_{12}(XA-\Delta)(XB-\Delta)]\div[(\beta-\Delta)(\Gamma-\Delta)(\alpha-\Gamma)]$$
$$E = [(\text{dose/volume})(k_{12}k_{23})(k_{43}-\alpha)]\div[(\beta-\alpha)(\Gamma-\alpha)(\Delta-\alpha)]$$
$$F = [(\text{dose/volume})(k_{12}k_{23})(k_{43}-\beta)]\div[(\alpha-\beta)(\Gamma-\beta)(\Delta-\beta)]$$
$$G = [(\text{dose/volume})(k_{12}k_{23})(k_{43}-\Gamma)]\div[(\alpha-\Gamma)(\beta-\Gamma)(\Delta-\Gamma)]$$
$$H = [(\text{dose/volume})(k_{12}k_{23})(k_{43}-\Delta)]\div[(\alpha-\Delta)(\beta-\Delta)(\Gamma-\Delta)]$$
$$I = (E)(k_{34})\div(k_{43}-\alpha)$$
$$J = (F)(k_{34})\div(k_{43}-\beta)$$
$$K = (G)(k_{34})\div(k_{43}-\Gamma)$$
$$L = (H)(k_{34})\div(k_{43}-\Delta)$$
$$XA = \tfrac{1}{2}\{(k_{43}+k_{32}+k_{34}+k_{30}) + [(k_{43}+k_{32}+k_{34}+k_{30})^2 - 4(k_{43})(k_{32}+k_{30})]^{1/2}\}$$
$$XB = \tfrac{1}{2}\{(k_{43}+k_{32}+k_{34}+k_{30}) - [(k_{43}+k_{32}+k_{34}+k_{30})^2 - 4(k_{43})(k_{32}+k_{30})]^{1/2}\}$$
$$\alpha = k_{12} + k_{10}$$
$$\beta = S - T + P/3$$
$$\Gamma = \frac{S+T}{2} - \frac{S-T}{2}\sqrt{-3} + (P/3)$$
$$\Delta = \frac{S+T}{2} + \frac{S-T}{2}\sqrt{-3} + (P/3)$$
$$P = k_{23} + k_{32} + k_{34} + k_{43} + k_{30}$$
$$Q = 2(k_{43}k_{23}) + (k_{43}k_{30}) + (k_{23}k_{34}) + (k_{23}k_{30})$$
$$R = (k_{23}k_{43}k_{30})$$
$$S = \left[-b/2 + \left(\frac{b^2}{4} + \frac{a^3}{27}\right)^{1/2}\right]^{1/3}$$
$$T = \left[-b/2 - \left(\frac{b^2}{4} + \frac{a^3}{27}\right)^{1/2}\right]^{1/3}$$
$$a = (1/3)(3Q - P^2)$$
$$b = (1/27)(2P^3 - 9PQ + 27R)$$

The magnitude of the first-order constants associated with drug disposition in the eye are:

microconstants	minutes^{-1}
k_{10}	5.71×10^{-1}
k_{12}	6.2×10^{-3}
k_{23}	4.85×10^{-2}
k_{32}	4.03×10^{-2}
k_{34}	8.89×10^{-3}
k_{43}	3.39×10^{-3}
k_{30}	3.49×10^{-2}

REFERENCES

(1) R. Lazare and H. Horlington, *Exp. Eye Res.*, **21**, 281 (1975).

(2) M. D. Van Hoose and F. E. Leaders, *Invest. Ophthalmol.*, **13**, 377 (1974).

(3) S. Yoshida and S. Mishima, *Jpn. J. Ophthalmol.*, **19**, 121 (1975).

(4) J. W. Sieg and J. R. Robinson, *J. Pharm. Sci.*, **64**, 931 (1975).

(5) K. Green and D. L. MacKeen, *Invest. Ophthalmol.*, **15**, 220 (1976).

(6) H. Beasley, J. J. Boltralik, and H. A. Baldwin, *Arch. Ophthalmol.*, **93**, 184 (1975).

(7) J. Y. Massey, C. Hanna, R. Goodart, and T. Wallace, *Am. J. Ophthalmol.*, **81**, 151 (1976).

(8) R. E. Hardberger, C. Hanna, and R. Goodart, *ibid.*, **80**, 133 (1975).

(9) T. F. Patton, Ph.D. thesis, University of Wisconsin, Madison, Wis., 1975.

(10) S. S. Chrai and J. R. Robinson, *Am. J. Ophthalmol.*, **77**, 735 (1974).

(11) K. A. Connors, "A Textbook of Pharmaceutical Analysis," Wiley, New York, N.Y., 1967, p. 502.

(12) P. Chung, T. Chin, and J. Lach, *J. Pharm. Sci.*, **59**, 1300 (1970).

(13) L. Sendelbeck, D. Moore, and J. Urquhart, *Am. J. Ophthalmol.*, **80**, 214 (1975).
(14) S. S. Chrai, M. C. Makoid, S. P. Eriksen, and J. R. Robinson, *J. Pharm. Sci.*, **63**, 333 (1974).
(15) S. S. Chrai, T. F. Patton, A. Mehta, and J. R. Robinson, *ibid.*, **62**, 1112 (1973).
(16) J. W. Sieg and J. R. Robinson, *ibid.*, **65**, 1816 (1976).
(17) R. E. Notari, J. E. DeYoung, and R. H. Reuning, *ibid.*, **61**, 135 (1972).
(18) D. Perrier and M. Gibaldi, *ibid.*, **62**, 225 (1973).
(19) L. J. Leeson and H. Weintraub, *ibid.*, **62**, 1936 (1973).
(20) M. C. Makoid, J. W. Sieg, and J. R. Robinson, *ibid.*, **65**, 150 (1976).
(21) J. S. Lyons and D. L. Krohn, *Am. J. Ophthalmol.*, **75**, 885 (1973).
(22) D. M. Maurice, *The Sight Saving Review*, **42**, 42 (1972).

ACKNOWLEDGMENTS

Supported by a grant from Allergan Pharmaceuticals, Irvine, CA 92664, and by Grant EY-01332 from the National Institutes of Health.
The authors thank Mr. Arthur Welnitz for technical assistance.

Rapid Determination of Theophylline in Serum by Electron-Capture GLC

SY-RONG SUN

Received July 13, 1978, from the *Pharmaceutical Products Division, Abbott Laboratories, North Chicago, IL 60064.* Accepted for publication September 11, 1978.

Abstract □ A rapid and sensitive GLC procedure was developed for the determination of theophylline in serum. After extraction from serum with ethyl acetate, theophylline and the internal standard were derivatized with pentafluorobenzyl bromide under alkaline conditions. The derivatives were quantitated by electron-capture detection. The method has a sensitivity of 0.1 μg/ml with a 0.1-ml serum sample.

Keyphrases □ Theophylline—electron-capture GLC determination of serum levels □ GLC, electron capture—analysis, theophylline in serum □ Relaxants, smooth muscle—electron-capture GLC analysis of theophylline in serum

Methods for the determination of theophylline in biological fluids are based on spectrophotometry (1–3), GLC (4–8), TLC (9), and high-pressure liquid chromatography (10–14). Recently, an electron-capture GLC procedure was reported (15) that involves the extraction of theophylline and the internal standard, theobromine, into methylene chloride by elution through a cellulose column. The compounds are then back-extracted into an alkaline aqueous phase and derivatized with pentafluorobenzyl bromide by extractive alkylation. The derivatives are separated from excess reagent by solvent extraction and finally determined by electron-capture GLC. This method is tedious, and the use of theobromine as an internal standard is not a good choice because it is present in beverages such as tea and cocoa and is a metabolite of caffeine (16–18).

The present, rapid method requires only 0.1-ml serum sample. It involves one-step extraction of the serum sample with ethyl acetate, followed by derivatization with pentafluorobenzyl bromide under alkaline conditions at 100°. Excess reagent is removed by evaporation. A chemical isomer of theophylline, which is not present in beverages and is not a metabolite of caffeine, is used as the internal standard. The sensitivity of the assay is 0.1 μg/ml with a 0.1-ml serum sample.

EXPERIMENTAL

Reagents and Materials—Theophylline[1], the internal standard (5,7-dimethyl-2*H*-pyrazolo[3,4-*d*]pyrimidine-4,6-(5*H*,7*H*)-dione, I)[2], and pentafluorobenzyl bromide[3] were used as supplied. The other chemicals were analytical reagent grade.

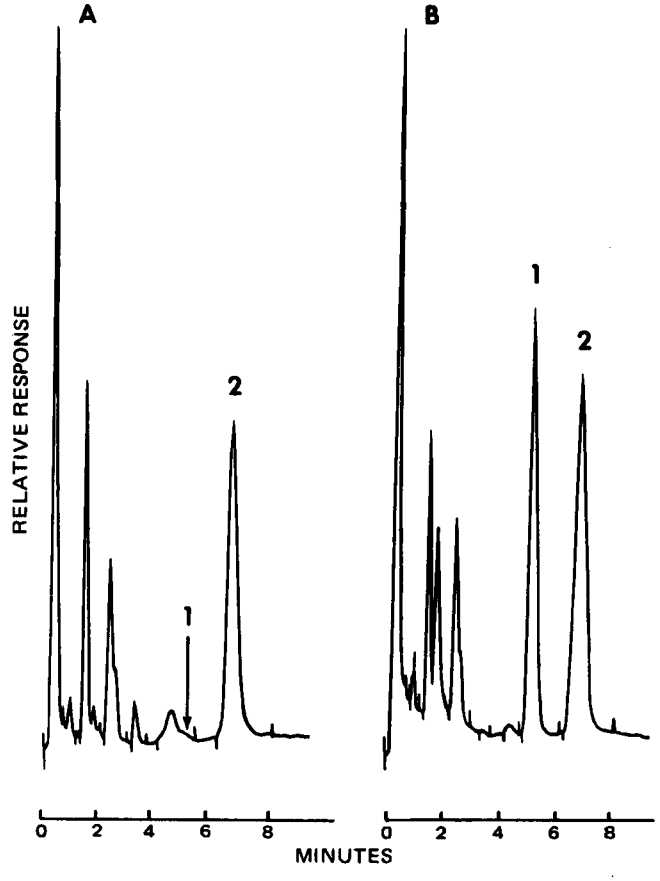

Figure 1—*GLC tracings of extracted serum samples. Key: A, serum blank containing the internal standard; B, serum standard containing the internal standard and theophylline at 5 μg/ml serum; 1, theophylline; and 2, internal standard.*

[1] Theophylline USP ($C_7H_8N_4O_2 \cdot H_2O$).

[2] Nippons Shinyaku Co., Kyoto, Japan.
[3] Pentafluorobenzyl bromide, Pierce Chemical Co., Rockford, Ill.

0022-3549/79/0400-0443$01.00/0